

Anticorrosive properties of styrene-acrylic resins containing aluminum tripolyphosphate

Lin-Jian SHANGGUAN – School of Mechanical Engineering, North China University of Water Conservancy and Electric Power, Zhengzhou 450011, China; Wugang MA, Guoqin LIU*, Weiqiang SONG – College of Material Science and Engineering, Henan University of Technology, Zhengzhou, 450000, China

Please cite as: CHEMIK 2015, 69, 9, 578–585

Introduction

Emulsion polymerization is widely used to produce water-based resins with various colloidal and physicochemical properties [1–4]; the reaction medium is usually water, which facilitates agitation and mass transfer, and provides an inherently safe process; moreover the process is environmentally friendly.

Styrene acrylic emulsion is widely applied in the area of coating and adhesive for its prominent properties such as good durability, availability at low cost, compatibility with other materials, excellent adhesive characteristic, and ability to form continuous film upon drying of the emulsions, high resistance to UV light, oxygen, water, various types of solvents and excellent durability [5, 6]. However, styrene-acrylic emulsion-based polymer provides little anticorrosion property. It seems reasonable to prepare styrene acrylic emulsion-based composites for building anticorrosion materials by incorporating anticorrosion pigment.

Traditional anticorrosive paints contain lead or chromium compounds as active pigments; however, these pigments lead to the environmental pollution and, meanwhile, pose a risk to human health. One of the leading substitutes for these classic pigments is the inorganic tripolyphosphate, which constitutes a promising group of nontoxic phosphate corrosion inhibitors for paints. Among them, aluminum tripolyphosphate ($\text{AlH}_2\text{P}_3\text{O}_{10}\cdot 2\text{H}_2\text{O}$: ALP) has been developed and used widely as an anticorrosion pigment due to its low toxicity to humans and environment, and better anticorrosive properties.

In this study, we synthesised a styrene-acrylic emulsion composite with ALP for anticorrosion resins. The structural characteristics, distribution and particles size and anticorrosion performance of styrene-acrylic resins/aluminum tripolyphosphate coatings were investigated. In addition, to study the effect of ALP on final properties of coatings, the coatings with no pigment (blank coating), calcium tripolyphosphate ($\text{Ca}_5(\text{P}_3\text{O}_{10})_2$: CAP) and zinc phosphate ($\text{Zn}_3(\text{PO}_4)_2$: ZNP) were employed as references.

Experimental

Materials

Styrene(St), methacrylic acid (MAA) and ethylacrylate (EA) were all the analytical reagent and purchased from Shanghai Chemicals Inc.; the inhibitor can be removed prior to polymerization by shaking with 10% aqueous NaOH, washing with water and drying over Na_2SO_4 and then they were distilled under reduced pressure before use and stored at -4°C . Potassium persulfate (KPS), NaHCO_3 and sodium dodecyl sulfate (SDS) were respectively used as initiator, buffer and emulsifier, purchased from Beijing Fine Chemicals Inc. Ltd. and used as received. Distilled water was obtained by distillation. ALP, CAP and ZNP were analytical grades and used directly without further purification.

Preparation of styrene-acrylic emulsion

Emulsion copolymerization was carried out using a 500 mL 4-necked round bottom flask equipped with a reflux condenser, stainless steel stirrer, and two separate feed streams. The first feed stream was a solution of St, EA, and MAA. The other feed was the initiator solution (1 wt%). Before emulsion polymerization began, the reaction vessel was first charged with the desired amounts of distilled water, emulsifier, and NaHCO_3 , respectively. During polymerization process, the temperature was maintained at 65°C ; the monomer mixture was added to the flask at a period of 120 min under N_2 atmosphere. A typical composition of the preparation of a 32% solid product was given in Table I.

Table I

Composition of polymerization at 65°C

Component	Total
St (g)	19.5
MAA (g)	7.5
EA (g)	3
NaHCO_3 (g)	0.6
KPS (g)	0.2
SDS (g)	1.5
H_2O (g)	170

Preparation of anticorrosive coated samples

ALP, anti-settling agent and dispersant were incorporated; all mixtures were dispersed for 24h in the vehicle, employing a ball mill, to achieve an acceptable dispersion degree; distilled water was employed as solvent; the styrene-acrylic resins/ALP ratio was 100/15, 100/10, and 100/5 (w/w) respectively; styrene-acrylic emulsion containing ALP was prepared in a high-speed disperser. The paint was coated on one surface of steel panels with dimensions of $120\text{ mm} \times 100\text{ mm} \times 4\text{ mm}$ by brushing to a thickness of $100\mu\text{m}$, and air-dried at room temperature for 3 d. Meanwhile, the blank coating, the styrene-acrylic resins/CAP, (100/5 w/w) and the styrene-acrylic resins/ZNP (100/5 w/w) were also prepared using the same method.

Measurements

FT-IR spectroscopic analysis Infrared spectra were recorded using a Perkin-Elmer spectrum-2000 spectrometer. Samples were prepared by grinding the dried polymers with KBr and compressing the mixtures to form disks. Latex particle size analysis was performed on laser particle size analyzer (a Microtrac S3000 analyzer, USA), a certain quantity of final emulsion was diluted properly by distilled

Corresponding author:

Guoqin LIU – Ph.D., Eng, Associate Professor, e-mail: liugq1970@126.com

water. The adhesion property of the coatings was measured according to ASTM D3359 before and after salt spray test while the salt spray test carried out according to ASTM B117 and analyzed using ASTM D1654 standard. Electrochemical impedance spectroscopy (EIS) was used to assess the anticorrosive properties of the coating of styrene-acrylic emulsion containing ALP. EIS measurements were performed using RST5000 Electrochemical Station. The coated samples were immersed in a 10% NaCl solution. A classical three-electrode system including a saturated calomel electrode as a reference electrode, the coated sample as a working electrode and platinum as a counter electrode was applied, as shown in Figure 1. A sine wave of 10 mV was applied across the cell. The measurements were made in the frequency range of 50 kHz-0.1 Hz.

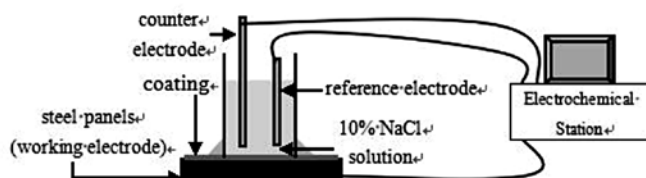


Fig. 1. Schematic diagram of EIS measurements

Results and discussion

In emulsion polymerization, the size and distribution of the latex particles has a great impact on the performance of its applications of the emulsion, and also reflects the emulsion polymerization process. Various industrial products, which require a different particle size of the latex, can be prepared according to industry needs [7 – 9]. Due to many advantages of the styrene-acrylic emulsion and its wide range of applications, styrene-acrylic emulsion has been developed and improved.

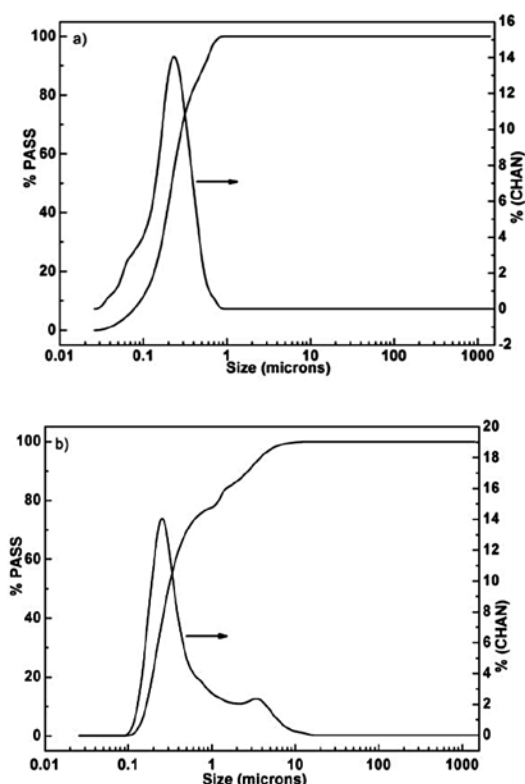


Fig. 2. The size distribution of a) styrene-acrylic resins and b) styrene-acrylic resins/ALP

The diameter distribution of prepared styrene-acrylic resins and styrene-acrylic resins/ALP (100/15) was measured, as shown in Figure 2. It could be seen that the particle size of styrene-acrylic latex particles almost uniformly distributed from 36 nm to 688 nm with the D50 value of 218 nm, as shown in Figure 2 a); however, for

styrene-acrylic emulsion/ALP, it was found that the D50 value of the particle size increased to 1.44 μm , as shown in Figure 1 b), and the agglomeration process occurred in the styrene-acrylic resins/ALP; this could only be explained by partly ALP particles which had an influence on the distribution of latex particles.

FTIR is an important in studying the copolymer structure. The width and intensity of the spectrum bands, as well as the position of the peaks confirmed the functional groups that took part in the formation of copolymer. Styrene-acrylic resins, ALP and styrene-acrylic resins/ALP (100/15) in this study were shown in Figure 3.

For styrene-acrylic resins, characteristic absorption bands were clearly visible at 3349 cm^{-1} corresponding to the -OH stretching vibrations, this band was due to the stretching vibrations of free -OH groups. A band at 1259 cm^{-1} due to the -OH bending vibration. C-C and C-O stretching vibration were observed at 1169 cm^{-1} and 1028 cm^{-1} , respectively. The sharp band at 1730 cm^{-1} corresponded to the C=O stretching of the carbonyl group. The corresponding bending and wagging of -CH vibrations was at 1434 cm^{-1} and 1374 cm^{-1} , respectively; the C-H aromatic stretching vibration was observed between 3100 cm^{-1} and 2900 cm^{-1} ; C-H aliphatic stretching at 2977 cm^{-1} , 2919 cm^{-1} and 2847 cm^{-1} ; C-O stretching at about 1725 cm^{-1} ; a sharp absorption at 1495 cm^{-1} and a shoulder around 1584 cm^{-1} due to skeletal C-C aromatic stretching; aromatic C-H out-of-plane bending around 757 cm^{-1} and 700 cm^{-1} .

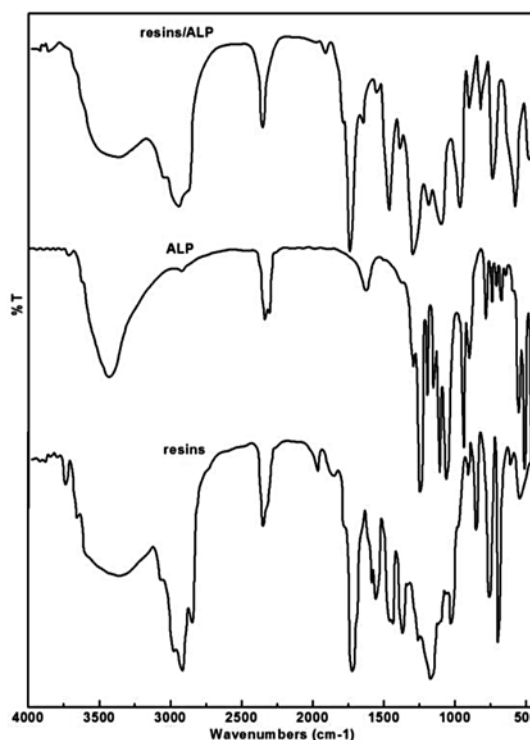


Fig. 3. FTIR spectrum of styrene-acrylic resins, ALP and styrene-acrylic resins/ALP

For ALP, according to literature [10 – 12], $(\text{H}_2\text{PO}_4)^{2-}$ anion possessed two types of distances: P-OH terminal due to the $\text{P}(\text{OH})_2$ groups, and P-O terminal attributed to the PO_2 . Therefore, the band assignments in infrared spectra could be made in terms of the $\text{P}(\text{OH})_2$, PO_2 and O-H vibrations; the terminal stretching modes of $(\text{H}_2\text{PO}_4)^{2-}$ anions usually occurred in the region 1250-870 cm^{-1} ; two bands were observed at 1059 cm^{-1} and 1114 cm^{-1} (symmetric mode corresponding to PO_2) and 1156 cm^{-1} (antisymmetric mode corresponding to PO_2); the asymmetric stretching vibrations of $\text{P}(\text{OH})_2$ groups gave the strong band at 936 cm^{-1} ; the band at 901 cm^{-1} were due to the vibrations of P-OH mode.

For styrene-acrylic resins/ALP (100/15), IR absorption at 2942 cm^{-1} was characteristic of C-H aliphatic stretching. The characteristic IR

absorption of carbonyl group was at 1730 cm^{-1} . The peak at 964 cm^{-1} was characteristic of $\text{P}(\text{OH})_2$ group. The stretching vibration absorption of $\text{P}-\text{OH}$ mode was at 903 cm^{-1} ; the two bands of PO_2 vibrations were overlapped with $\text{C}-\text{O}$ stretching vibration of styrene-acrylic resins at 1028 cm^{-1} . Disappearance of the peak at $1,660\text{ cm}^{-1}$ showed that $\text{C}=\text{C}$ bonds participated in polymerisation. The above discussion confirmed that the newly synthesized styrene-acrylic resins/ALP latex were mixtures of styrene-acrylic emulsion and ALP.

Organic coatings can provide corrosion protection by separating the corrosive environment from the steel. In general, a coating needs to have good barrier properties to provide good protection, i.e. a low permeability to water, ions, dissolved gases, and other corrosives; highly protective coatings with good barrier properties have a high electrical resistance. EIS is a quantitative and effective method for evaluating anticorrosion performance of organic coatings, which is widely characterized the protective properties of organic coatings on metal. When the coating is exposed to real or simulated service conditions, its impedance gradually decreases. The rate of decrease is a function of the coating formulation and the severity of the service conditions. Finally the impedance will drop to the point where coating permeability to water is very high and corrosion protection is lost.

In this study, the anticorrosive properties of styrene-acrylic resins and styrene-acrylic resins/ALP were investigated. The coating resistance as a function of time during the immersion in 10% NaCl solution was shown in Figure 4. The initial impedance and the decrease in impedance as a function of time were used to assess coating protection and deterioration. The way the impedance changes with time enabled a better prediction of long-term performance of the coating. The higher impedance means better anticorrosion effect.

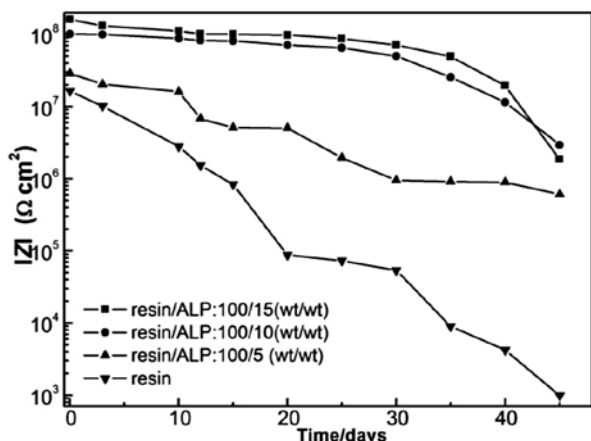


Fig. 4. Coating impedance as a function of time at 65°C

It is shown in Figure 4 that the resistance of the coatings with aluminum tripolyphosphate pigment at 0.1 Hz was higher than $10^8\ \Omega$ at the beginning of exposure to 10% NaCl solution at 65°C and, for the coating of styrene-acrylic resin/ALP ratio 100/15 and 100/10, it still maintained above $10^8\ \Omega\cdot\text{cm}^2$ after 15 d of exposure; the coatings had relatively high impedance, typical of high performance coatings. However, its impedance dropped consistently with time; it showed a small decrease to $10^7\ \Omega\cdot\text{cm}^2$ after 40 d; the decrease in resistance at the initial stage of exposure might be due to the permeation of water and ions into the film. For the coating of resin/ALP ratio 100/5, at the beginning of exposure, the resistance at 0.1 Hz was around $1.6 \times 10^7\ \Omega\cdot\text{cm}^2$. and it decreased continuously to above $10^5\ \Omega\cdot\text{cm}^2$ until 40 d of exposure.

In the case of styrene-acrylic resins, as shown in Figure 4, the resistance at 0.1 Hz was higher than $10^7\ \Omega\cdot\text{cm}^2$ up to the first 3 d of exposure. However, it decreased quickly to $10^5\ \Omega\cdot\text{cm}^2$ at 15 d. After 40 d of exposure, a few blisters were found on the specimen and the resistance was about $10^3\ \Omega\cdot\text{cm}^2$. A general consensus is that

the coatings with a resistance higher than $10^8\ \Omega\cdot\text{cm}^2$ reveals good anticorrosive performance, while that with the resistance lower than $10^6\ \Omega\cdot\text{cm}^2$ has weak anticorrosive properties. So the styrene-acrylic resins coating lost its anticorrosive properties within the first 15 d of exposure.

From the comparison of results for styrene-acrylic resins/ALP and styrene-acrylic resins films, it could be seen that ALP pigments enhanced the anticorrosive properties of coating.

The steel plates coated by the styrene-acrylic resins and the styrene-acrylic resins/ALP were exposed to salt spray test medium for 40 days. Visual investigation of corrosion confirmed the existence of the areas with blisters and corrosion products on top of coating film for the styrene-acrylic resins; the rusted points and disbanding film could be observed on the surface. The white spots which was clearly observable on the surface of the sample indicated the diffusion of water, oxygen and corrosive ions such as chlorine through the coating to reach to the metal-coating interface to form corrosion products. In case of the coating made by styrene-acrylic resins/ALP, there was no blister or rust on the coating surface after 40 days in salt spray test.

Table 2

The results of adhesion test according to ASTM D 3359

Coating	Result	
	Before salt spray	After salt spray
styrene-acrylic resins	5B	3B
resins/ALP (100/5)	5B	5B
resins/ALP (100/10)	5B	5B
resins/ALP (100/15)	5B	5B

Investigating the coating appearance according to ASTM D1654 showed the presence of No.6 (medium) blisters and rusted points around the scratched area for the styrene-acrylic resins. On the other hand for styrene-acrylic resins/ALP, there was no blister or rust. The adhesion properties of coatings were investigated using adhesion test according to ASTM D3359 method. Table 2 showed the results of adhesion test before and after 40 days exposure time to salt spray atmosphere. According to these results, the adhesion properties of styrene-acrylic resins decreased from 5B to 4B; in contrast, styrene-acrylic resins/ALP did not show considerable changes in adhesion after 40 days being in salt spray test. These results showed that the adhesion and anti-corrosion properties of styrene-acrylic resins coatings were obviously improved by adding ALP.

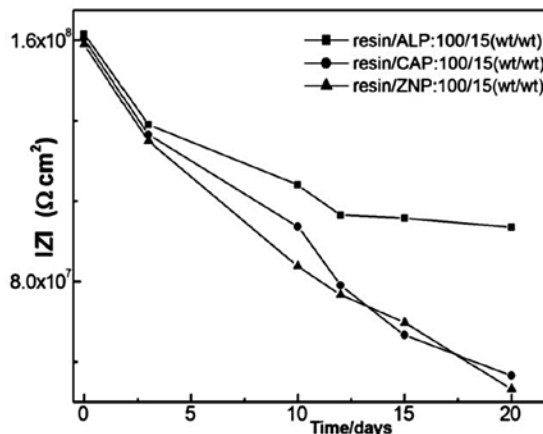


Fig. 5. Coating impedance as a function of time with ALP, CAP, and ZNP pigments at 65°C

In this study, the anticorrosive behaviors of coatings containing ALP, CAP, and ZNP pigments were also investigated by means of

electrochemical impedance method. The coating resistance as a function of time during the immersion in 10% NaCl solution is shown in Figure 5. It can be seen that the resistance of the three coatings were higher than $10^8 \Omega \cdot \text{cm}^2$ at the beginning of exposure; styrene-acrylic resins/CAP and styrene-acrylic resins/ZNP composite coatings decreased to $7.8 \times 10^7 \Omega \cdot \text{cm}^2$ after 10 d of exposure and decreased continuously to $4.8 \times 10^7 \Omega \cdot \text{cm}^2$ until 20 d of exposure. For styrene-acrylic resins/ALP, it showed a small increase to $9.8 \times 10^7 \Omega \cdot \text{cm}^2$ until 20 d. It is generally known that the coating films with the resistance lower than $10^6 \Omega \cdot \text{cm}^2$. Has poor anticorrosive properties, so, ALP, CAP, and ZNP pigments have good anticorrosive properties and, among them, aluminum tripolyphosphate showed the superior anticorrosive performance.

Conclusion

Aluminum tripolyphosphate were dispersed into styrene-acrylic emulsion through high-speed disperser, which could significantly improve the corrosion resistance of styrene-acrylic resins. The electrical resistance of the coatings containing the aluminum tripolyphosphate and the styrene-acrylic resins film was respectively above $10^6 \Omega \cdot \text{cm}^2$ and $4076 \Omega \cdot \text{cm}^2$ after 40 days of immersion in 10 wt% NaCl aqua corrosive solutions. The adhesion and anticorrosion properties of styrene-acrylic resins coatings were obviously improved by adding ALP.

Literature

1. Chaduc I., Crepet A., Boyron O., et al.: Effect of the pH on the RAFT polymerization of acrylic acid in water: application to the synthesis of poly (acrylic acid)-stabilized polystyrene particles by RAFT emulsion polymerization. *Macromolecules*, 2013, **46**, 6013-6023.
2. Kniajanski S., Colborn R. E., Bales B. C., et al.: Synthesis of highly loaded and well-controlled magnetic beads via emulsion polymerization. *J. Appl. Polym. Sci.* 2013, **129**, 1726-1733.
3. Rozik N., Antonietti M., Yuan J., et al.: Polymerized ionic liquid as stabilizer in aqueous emulsion polymerization enables a hydrophilic-hydrophobic transition during film formation. *Macromol. Rapid. Comm.* 2013, **34**, 665-671.
4. Naghash H. J., Mallakpour S., Kayhan N.: Synthesis and characterization of silicone modified acrylic resin and its uses in the emulsion paints. *Iran. Polym. J.* 2005, **14**, 211-222.
5. Zhou C., Wu S., Liu H., Wu, G.: Effects of core-shell particle growth manners on morphologies and properties of poly(vinyl chloride)/(methyl methacrylate-butadiene-styrene) blends. *J. Vinyl. Addit. Technol.* 2014, **20**, 21438.

6. Wang P. H., Pan C. Y.: Preparation of styrene/acrylic acid copolymer microspheres: polymerization mechanism and carboxyl group distribution. *Colloid Polym. Sci.* 2002, **280**, 152-159.
7. Amaral M. do., Roos A., Asua J. M., Creton C.: Assessing the effect of latex particle size and distribution on the rheological and adhesive properties of model waterborne acrylic pressure-sensitive adhesives films. *J. Colloid. Interf. Sci.* 2005, **281**, 325-338.
8. Tiarks F., Frechen T., Kirsch S., et al.: Formulation effects on the distribution of pigment particles in paints. *Prog. Org. Coat.* 2003, **48**, 140-152.
9. Brown R. F. G., Carr C., Taylor M. E.: Effect of pigment volume concentration and latex particle size on pigment distribution. *Prog. Org. Coat.* 1997, **30**, 185-194.
10. Deyá M., Di Sarli A. R., del Amo B., Romagnoli R.: Performance of anticorrosive coatings containing tripolyphosphates in aggressive environments. *Ind. Eng. Chem. Res.* 2008, **47**, 7038-7047.
11. Koleva V., Stefov V., Cahil A., Najdoski M., Šoptrajanov B., Engelen B., Lutz H. D.: Infrared and Raman studies of manganese dihydrogen phosphate dihydrate, $\text{Mn}(\text{H}_2\text{PO}_4)_2 \cdot 2\text{H}_2\text{O}$. I: Region of the vibrations of the phosphate ions and external modes of the water molecules. *J. Mol. Struct.* 2009, **917**, 117-124.
12. Koleva V., Stefov V., Cahil A., Najdoski M., Šoptrajanov B., Engelen B., Lutz H. D.: Infrared and Raman studies of manganese dihydrogen phosphate dihydrate, $\text{Mn}(\text{H}_2\text{PO}_4)_2 \cdot 2\text{H}_2\text{O}$. Part II: Region of the internal OH group vibrations. *J. Mol. Struct.* 2009, **919**, 164-169.

Professor Lin-Jian SHANGGUAN – Ph.D., Eng.. He obtained an academic degree of doctor in 2012 and was awarded the title of the Associate Professor in 2013. He is the author and co-author of over 28 China and foreign publications.

*Guoqin LIU – Ph.D., Eng, Associate Professor obtained a university degree in 1994. He obtained an academic degree of doctor in 2005 and was awarded the title of the Associate Professor in 2007. Dr G. LIU is a member of the Chinese Chemical Society. He is the author and co-author of over 25 China and foreign publications.
e-mail: liuq1970@126.com, phone: +86-13513896470

Professor Weiqiang SONG – Ph.D., Eng.. Prof. SONG is a member of the Chinese Chemical Society. He is the author and co-author of over 30 China and foreign publications.

Aktualności z firm

News from the Companies

Dokończenie ze strony 581

Spotkanie Premier Ewy Kopacz z przedstawicielami środowiska naukowego

W nawiązaniu do listu Konferencji Rektorów Akademickich Szkół Polskich, Polskiej Akademii Nauk, Narodowego Centrum Nauki oraz Rady Głównej Nauki i Szkolnictwa Wyższego r., przedstawiającego konieczność zwiększenia finansowania badań naukowych, 25 sierpnia br. w Kancelarii Prezesa Rady Ministrów odbyło się spotkanie Premier Ewa Kopacz z przedstawicielami środowiska naukowego.

W spotkaniu udział wzięli: Minister NiSW, prof. Lena Kolarska-Bobińska, wice-minister NiSW, prof. Marek Ratajczak, rzecznik prasowy Rządu, Cezary Tomczyk, przewodniczący KRASP, rektor Uniwersytetu Śląskiego, prof. Wiesław Banyś, prezes PAN, prof. Jerzy Duszyński,

przewodniczący Rady NCN, prof. Michał Karoński, przewodniczący RGNiSzW, prof. Jerzy Woźnicki, prezes Zarządu Fundacji na Rzecz Nauki Polskiej, prof. Maciej Żylicz, wice-przewodniczący KRASP, rektor Politechniki Łódzkiej, prof. Stanisław Bielecki, przewodniczący Konferencji Rektorów Uniwersytetów Polskich, rektor Uniwersytetu im. A. Mickiewicza w Poznaniu, prof. Bronisław Marciniak, przewodniczący Komisji ds. Organizacyjnych i Legislacyjnych KRASP, rektor Uniwersytetu Warszawskiego, prof. Marcin Pałys, rektor Szkoły Głównej Handlowej, prof. Tomasz Szapiro.

Spotkanie poświęcone było omówieniu stanu i perspektyw finansowania nauki i szkolnictwa wyższego przed zbliżającymi się decyzjami w sprawie kształtu przyszłorocznego budżetu. (kk)

(<http://www.aktualnosci.pan.pl/>, 28.08.2015)

Dokończenie na stronie 588